Study on the single-event burnout mechanism of GaN MMIC power amplifiers

Hao Zhang,[1] Xuefeng Zheng,[1,a)] Danmei Lin,[1] Ling Lv,[1] Yanrong Cao,[1] Yuehua Hong,[1] Fang Zhang,[1] Xiaohu Wang,[1] Yingzhe Wang,[1] Weidong Zhang,[2] Jianfu Zhang,[2] Xiaohua Ma,[1] and Yue Hao[1]

[1]*State Key Lab of Wide-Bandgap Semiconductor Devices, School of Microelectronics, Xidian University, Xi'an 710071, People's Republic of China.*

[2]*The School of Engineering, Liverpool John Moores University, L3 3AF Liverpool, U.K.*

In this letter, the single-event burnout (SEB) mechanism in gallium nitride (GaN) microwave monolithic integrated circuit (MMIC) power amplifiers with a high linear energy transfer (LET) of 78.1 MeV • cm^2/mg has been investigated in detail for the first time. A typical SEB phenomenon was observed. With the aid of photon emission measurements (PEM) and scanning electron microscopy (SEM), it is found that catastrophic burnout occurs in the power-stage GaN HEMTs and the MIM capacitors, respectively. For the GaN HEMT, the incident heavy ions will generate electron-hole pairs within it, which can gain enough energy with the transverse high electric field. The high-energy electrons will collide with the lattice near the drain electrode and induce significant electron trapping, which will result in a significant longitudinal local electric field. When a critical electric field is achieved, catastrophic burnout occurs. For the MIM capacitor, the burnout is attributed to the single-event dielectric rupture via severe impact ionization or latent tracks when heavy ions strike it.

Gallium nitride (GaN) high electron mobility transistors (HEMTs) are emerging devices for RF and microwave power amplification due to their superior properties such as high output power, high efficiency, and high operating temperature. Moreover, its excellent radiation resistance makes it the ideal device for space applications in harsh environments.[1-7] In recent decades, GaN HEMTs have been employed in microwave monolithic integrated circuits (MMICs) design. Compared to GaAs MMICs, GaN MMICs exhibit more compact size, higher output power, and lower loss. Furthermore, GaN MMIC power amplifiers (PAs) can offer more radiation tolerance in systems with limited prime energy. These properties make GaN MMIC PAs the promising solution for satellite systems and telecommunication equipment operated at high frequency and high power in space.[2,5,8,9]

However, reliability issues caused by radiation effects are still observed in GaN-based devices, especially the single-event burnout effects (SEBs), which can lead to device burnout at a lower bias.[13-19,23-25] Up to date, some research on the SEB in GaN HEMTs has been reported. However, most of them focus on GaN-based power electronic devices.[3,10-27] These works have reported several different failure modes, including the permanent increase in leakage current and the burnout of gate-drain and drain-source. In terms of that, several failure mechanisms have been proposed, such as the enhancement charge collection and the significant charge amplification,[3,12,14-21] gate leakage caused by latent tracks,[10,11,22] oxygen and nitrogen vacancies,[13] single-event gate rupture,[25-27] etc. However, to the best of our knowledge, there is limited research on the SEB mechanism in GaN MMICs. Accordingly, the failure mechanism and the sensitive burnout position of SEB in the device are still not well known. In comparison with discrete GaN HEMTs, GaN MMICs include passive devices, especially the MIM capacitors. The dielectric within it may be broken due to single-event dielectric rupture (SEDR).[1,28,29] In addition, GaN MMICs operate at high voltage levels with pulse mode in some cases. It will induce a strong voltage overshoot much higher than the rated operation bias, which makes SEB more easily triggered. Furthermore, the degradation mechanism of GaN MMICs under the linear energy transfer (LET) above 75 MeV • cm^2/mg has not been reported to the best of our knowledge. Thus, understanding the SEB mechanism of GaN MMICs under heavy ion irradiation with high LET is very pressing needed for RF applications in space.

In this work, the SEB experiments with LET of 78.1 MeV • cm^2/mg were performed on GaN MMIC PAs for the first time. The burnout phenomenon under heavy ion irradiation was clearly observed. The failure mechanism was analyzed and two types of failure mechanisms were proposed with the aid of the SEM technique and TCAD simulation.

8.0-12.0 GHz two-stage GaN MMIC PAs with GaN-on-SiC MMIC process have been studied in this work. This process provides 0.40 μm gate-length AlGaN/GaN Schottky-HEMTs. The distance between G-S and G-D is 1.7 μm and 3.5 μm, respectively. The process also provides other passive devices, such as NiCr resistor, MIM capacitor, active layer GaN resistor, low loss microstrip lines, and through substrate via hole. The GaN MMIC PAs exhibited a saturated output power (P_{out}) of 44-45 dBm, an average power-added efficiency (PAE) of 37%, and an associated gain of 15 dB

within the band. The drain-source breakdown voltage exceeds 100 V.

In order to investigate the SEB effect, the GaN MMICs are irradiated by Ta ion having the LET value of 78.1 MeV • cm^2/mg with the energy of 1721.4 MeV. The ion flux is around 1×10^4 ions/cm^2·s with a total fluence of 1×10^6 ions/cm^2. During the irradiation, the MMICs were biased with the gate bias of -5 V. The drain bias increases from 30 V with the step of 10 V until the device burns out. The SEB experiments were carried out at the Heavy Ion Research Facility in Lanzhou, Chinese Academy of Sciences, and were performed at room temperature.

In order to accurately determine the SEB process, the gate, source, and drain currents during the irradiation were monitored, respectively. FIG. 1(a) shows the different leakage current components during irradiation with $V_{DS\text{-}Stress}$ = 30 V. It is observed that both the gate and drain leakage currents have a slight increase and agree well with each other. And the source leakage current is more than one order of magnitude lower than both of them. When the drain bias increases to 50 V, a similar procedure occurs, which is shown in FIG. 1(b).

In order to determine the burnout voltage under heavy ions irradiation, the drain bias is further increased to 60 V, which is shown in FIG. 1(c). It is clearly observed that both the drain and the source leakage current have a sudden increase and reach the preset current limit value soon, which indicates that the SEB is triggered and a leakage path is formed between the source and drain. In order to verify it, the leakage currents under the identical bias conditions without irradiation are also given in FIG. 1(d). It shows that no increase is observed for all leakage currents from different electrodes. It confirms that the failure of GaN MMICs under irradiation is mainly attributed to SEB rather than the applied electrical stress.

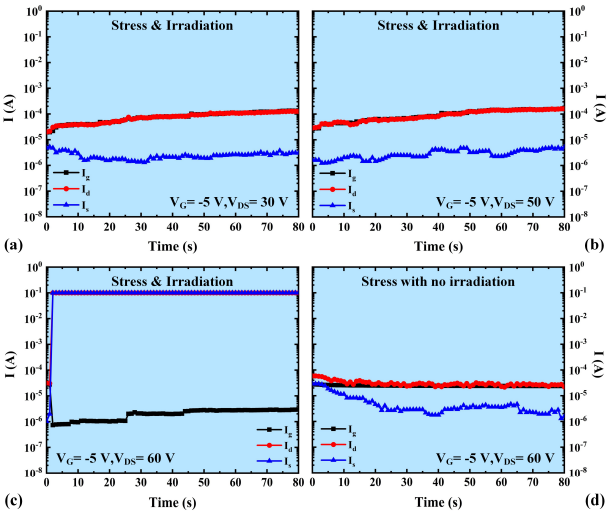

FIG. 1. Currents measured during the heavy ion irradiation with (a) $V_{DS\text{-}Stress}$ = 30 V, (b) $V_{DS\text{-}Stress}$ = 50 V, and (c) $V_{DS\text{-}Stress}$ = 60 V. (d) The currents of the reference MMICs under $V_{DS\text{-}Stress}$ = 60 V without irradiation. During the irradiation, the gate bias is kept at -5 V.

In order to have an in-depth study, the photon emission measurements (PEM) technique was utilized in this work to locate the failure point. FIG. 2(a) shows the photoemission signature of the fresh MMIC. It is clearly observed that there are few hotspots, indicating the absence of leakage paths. FIG. 2(b) shows some photoemission signature occurs in the irradiated MMIC with the drain bias of 30 V, which indicates that some faint local damages were generated. These damages are located in the GaN HEMTs rather than passive devices. When the drain bias increases to 50 V, more light distributions are observed, and the light emission intensities become stronger in FIG. 2(c), which indicates that the damage induced by heavy ions becomes more obvious. When the drain bias increases further to 60 V, a large range of photoemission signatures are observed in FIG. 2(d). It reveals a significant rise in the leakage current of the MMIC after triggering SEB. There are two features that should be noted. First, nearly all hotspots are observed in the power-stage HEMTs instead of driver-stage ones in the MMICs, which demonstrates that the power-stage suffers more severe stress. Second, photoemission signatures are also observed in the MIM capacitor region, which indicates that some leakage paths are generated within the insulated dielectric in MIM capacitors. The above results indicate that the heavy ions irradiation under 60 V induced not only the power-stage HEMTs burnout but also the dielectric damage in MIM capacitors within GaN MMICs.

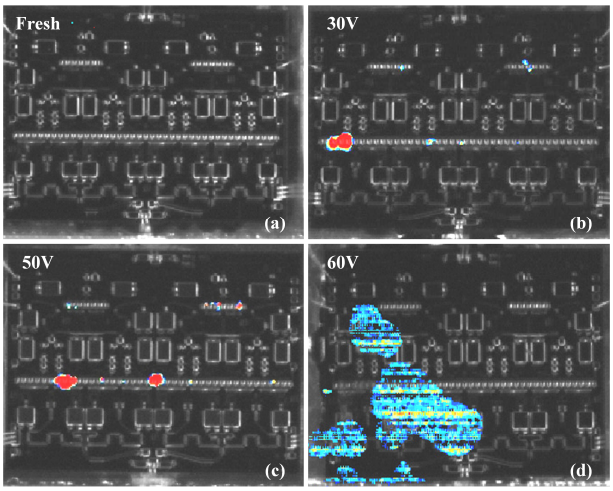

FIG. 2. PEM images of the fresh and irradiated GaN MMICs with different drain bias. (a) Fresh, (b) $V_{DS\text{-}Stress}$ = 30 V, (c) $V_{DS\text{-}Stress}$ = 50 V, and (d) $V_{DS\text{-}Stress}$ = 60 V.

In order to further investigate the physical origin of these leakage paths, the focused ion beam (FIB) and scanning electron microscopy (SEM) analysis were performed in this work. FIG. 3 shows the SEM photos for GaN HEMTs within the MMIC. As shown in FIG. 3(a), no damage is observed in the fresh device. However, a significant burnout was observed between the drain electrode and the substrate in the irradiated device with the drain bias of 60 V, as illustrated in FIG. 3(b). It should be noted that the other regions away from the drain electrode remain a relatively complete structure with little damage.

FIG. 4 shows the SEM photos for MIM capacitors within the MMIC. FIG. 4(a) shows the initial state of MIM capacitors, indicating it is almost free of any intrinsic crystal defects. FIG. 4(b) shows the morphology of the MIM capacitor after triggering SEB with the drain bias of 60 V. It can be seen that the dielectric layer and the top plate of the

capacitor are entirely burned out. In comparison, there is almost no damage or degradation was observed on MIM capacitors without irradiation at the identical bias voltage, which confirms the breakdown of MIM capacitors is attributed to single-event dielectric rupture.[28-30] When heavy ions irradiate MIM capacitors, dense electron-hole pairs can be induced in dielectric along the ion track. Under the influence of the high electric field across the MIM capacitor, the generated electrons and holes will be accelerated and become high-energy carriers. These high-energy carriers may induce significant leakage current via severe impact ionization, which can trigger the eventual burnout of the device. It is also possible that the latent tracks induced by the heavy ions strike induce leakage paths between the top plate and bottom plate, which leads to the final destruction of the dielectric.

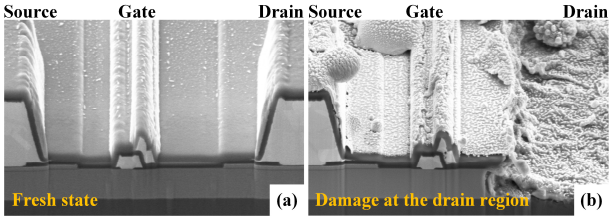

FIG. 3. SEM images show the morphology of GaN HEMTs in the MMICs under $V_{DS\text{-}Stress}$ = 60 V. (a) Fresh state. (b) The SEB damage at the drain region.

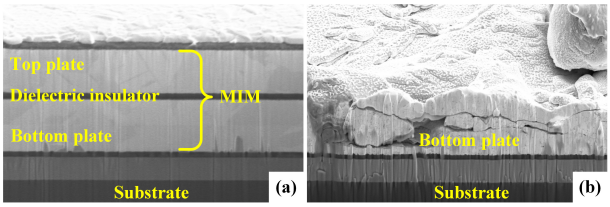

FIG. 4. SEM images show the morphology of MIM capacitors in the MMICs under $V_{DS\text{-}Stress}$ = 60 V. (a) Fresh state. (b) The morphology after SEB.

In order to have an in-depth understanding on the SEB mechanism in GaN HEMTs, TCAD simulation was carried out in this work. By simulating heavy ions striking at different positions from the source to the drain, it was found that SEB can be triggered more easily when heavy ions strike from the field plate edge. FIG. 5 demonstrates the hole and electron density distributions in GaN HEMT at different times after an ion strike at the field plate edge with the drain bias of 60 V. It can be seen that at 1×10^{-12} s, dense electron-hole pairs were induced along the ion track, as shown in FIG. 5(a) and (b). Then, these electrons and holes move towards the drain and gate electrodes driven by the transverse high electric field, respectively. Holes will accumulate below the gate due to the negative gate voltage, which can reduce the potential barrier between the source and the buffer, as shown in FIG. 5(c). As a result, electrons gradually begin to inject from the source to the drain at 2×10^{-11} s, as shown in FIG. 5(d). It will form an electron punch-through path and lead to the HEMT unexpectedly turning on, resulting in the leakage current from the drain to the source. In FIG. 5(e), when the time reaches 3×10^{-10} s, holes start to flow further towards the source. Meanwhile, more electrons are injected from the source to the drain, as shown in FIG. 5(f). Considering the significant transverse high electric field between the gate and drain, these injected electrons can be accelerated towards the drain electrode and become high-energy electrons, which can impact out more electron-hole pairs along the 2DEG channel, especially near the drain region. Most of electrons can be collected by the drain electrode and form drain current. The others will collide with the lattice in the GaN buffer layer near the drain region and generate new defects. Sequently, these electrons can get trapped within the newly generated defects and cause significant electron trapping. It is also possible that some of the high-energy electrons can surmount the interface barrier and inject into the AlGaN layer, which can form leakage current paths and cause potential damage. The above procedure is shown in FIG. 6(a).

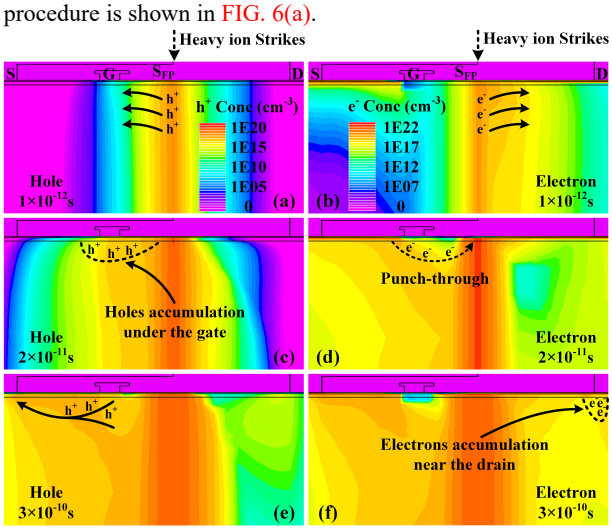

FIG. 5. (a), (c), (e) Hole and (b), (d), (f) Electron density distributions of HEMTs in GaN MMICs at various times after a heavy ion strike at the field plate edge.

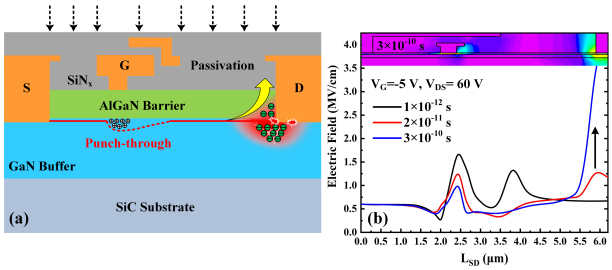

FIG. 6. (a) Schematic cross sections of GaN HEMTs in the MMICs show the electron trapping (Green solid symbols), and current leakage paths (Yellow arrow). (b) The simulated electric field in buffer layer at various times during heavy ion irradiation.

With the electron trapping within the buffer layer accumulates, the longitudinal electric field near the drain electrode will be modulated. The simulation results in FIG. 6(b) present it. It is observed that the electric field near the drain electrode increases dramatically after the heavy ion strike. When a critical longitudinal electric field (E_{Cr}) is achieved, a catastrophic burnout occurs near the drain region, which agrees well with the result observed in FIG. 3(b).

In conclusion, the SEB mechanism in GaN MMIC PAs with a high LET of 78.1 MeV • cm^2/mg has been studied for the first time in this work. When the drain bias increases to 60 V, a catastrophic burnout occurs with the drain current having a sudden increase. Utilizing PEM, it is found that both the

GaN HEMT and MIM capacitor contribute to SEB. With the aid of SEM, it is found that destructive damage happens near the drain electrode in GaN HEMT, which is explained by the local electric field modulate. The incident heavy ions can induce electron-hole pairs. With the transverse high electric field, high-energy electrons will be generated and new traps will be generated near the drain electrode. The sequential electron trapping within these traps leads to a critical breakdown electric field. The burnout in the MIM capacitor is attributed to SEDR through severe impact ionization or latent tracks. The results in this work can provide valuable information for the understanding of degradation mechanisms and reliability improvement in GaN MMICs.

This work was supported in part by the National Key R&D Program of China (Grant Nos. 2023YFB3611900 and 2021YFB3602404), in part by the National Natural Science Foundation of China (Grant Nos. U2241220, 61974115, 12035019 and 62234013), , and in part by the fund of National Innovation Center of Radiation Application (No. KFZC2022020401).

DATA AVAILABILITY

The data that support the findings of this study are available from the corresponding author upon reasonable request.

REFERENCES

[1]K. Hirche et al. (2014), [Online]. Available: https://escies.org/download/webDocumentFile?id=63411.

[2]A. R. Barnes, and F. Vitobello, *in Proc. 9th Eur. Microw. Integr. Circuit Conf.* (2014), 233.

[3]S. Kuboyama, A. Maru, H. Shindou, N. Ikeda, T. Hirao, H. Abe, and T. Tamura, IEEE Trans. Nucl. Sci 58(6), 2734-2738 (2011).

[4]D. S. Kim, J. H. Lee, S. Yeo, and J. H. Lee, IEEE Trans. Nucl. Sci 65(1), 579-582 (2018).

[5]R. S. Pengelly, S. M. Wood, J. W. Milligan, S. T. Sheppard, and W. L. Pribble, IEEE Trans. Microw. Theory Techn 60(6), 1764-1783 (2012).

[6]K. J. Chen, O. Häberlen, A. Lidow, C. L. Tsai, T. Ueda, Y. Uemoto, and Y. Wu, IEEE Trans. Electron Devices 64(3), 779-795 (2017).

[7]Z. Lei, H. Guo, M. Tang, C. Zeng, H. Chen, and Z. Zhang, *in Proc. 16th Eur. Conf. Radiat. Effects Compon. Syst* (2016), 46-49.

[8]A. Barigelli, W. Ciccognani, S. Colangeli, P. Colantonio, M. Feudale, F. Giannini, R. Giofrè, C. Lanzieri, E. Limiti, A. Nanni, A. Pantellini, and P. Romanini, *in Proc. 7th Eur. Microw. Integr. Circuits Conf* (2012), 369-372.

[9]A. Gurdal, B. A. Yilmaz, O. Cengiz, O. Sen, and E. Ozbay, *in Proc. 13th Eur. Microw. Integr. Circuits Conf* (2018), 345-348.

[10]S. Z. Yue, Z. Zhang, Z. Chen, X. Zheng, L. Wang, Y. M. Huang, Y. Huang, C. Peng, and Z. Lei, IEEE Trans. Electron Devices 68(6), 2667-2672 (2021).

[11]Z. F. Lei, H. X. Guo, M. T. Tang, C. Zeng, Z. G. Zhang, H. Chen, Y. F. En, Y. Huang, Y. Q. Chen, and C. Peng, Microelectron. Rel 80, 312-316 (2018).

[12]M. Zerarka, P. Austin, A. Bensoussan, F. Morancho, and A. Durier, IEEE Trans. Nucl. Sci 64(8), 2242-2249 (2017).

[13]Z. Islam, A. L. Paoletta, A. M. Monterrosa, J. D. Schuler, T. J. Rupert, K. Hattar, N. Glavin, and A. Haque, Microelectron. Rel 102, 113493 (2019).

[14]X. Luo, Y. Wang, Y. Hao, X. J. Li, C. M. Liu, X. X. Lei, C. H. Yu, and F. Cao, IEEE Trans. Electron Devices 66(2), 1118-1122 (2019).

[15]S. Onoda, A. Hasuike, Y. Nabeshima, H. Sasaki, K. Yajima, S.-i. Sato, and T. Ohshima, IEEE Trans. Nucl. Sci 60(6), 4446-4450 (2013).

[16]C. Abbate, G. Busatto, F. Iannuzzo, S. Mattiazzo, A. Sanseverino, L. Silvestrin, D. Tedesco, and F. Velardi, Microelectron. Rel 55(9-10), 1496-1500 (2015).

[17]Y. Liang, R. Chen, J. W. Han, X. Wang, Q. Chen, and H. Yang, Electronics 10(440), no. 440, 1-16 (2021).

[18]M. Rostewitz, K. Hirche, J. Lätti, and E. Jutzi, IEEE Trans. Nucl. Sci 60(4), 2525-2529 (2013).

[19]M. J. Martinez, M. P. King, A. G. Baca, A. A. Allerman, A. A. Armstrong, B. A. Klein, E. A. Douglas, R. J. Kaplar, and S. E. Swanson, IEEE Trans. Nucl. Sci 66(1), 344-351 (2019).

[20]S. M. Angulo, R. Rodríguez, J. D. Pino, B. González, and S. L. Khemchandani, Semicond. Sci. Technol 34(3), 1-8 (2019).

[21]Z. Zhen, C. Feng, Q. Wang, D. Niu, X. Wang, and Manqing Tan, IEEE Trans. Nucl. Sci 68(9), 2358-2366 (2021).

[22]P. P. Hu, J. Liu, S. X. Zhang, K. Maaz, J. Zeng, P. F. Zhai, L. J. Xu, Y. R. Cao, J. L. Duan, Z. Z. Li, Y. M. Sun, X. H. Ma, Nucl. Instrum. Methods Phys. Res. B 430(1), 59-63 (2018).

[23]E. Mizuta, S. Kuboyama, Y. Nakada, A. Takeyama, T. Ohshima, Y. Iwata, and K. Suzuki, IEEE Trans. Nucl. Sci 65(8), 1956-1963 (2018).

[24]L. Scheick, IEEE Trans. Nucl. Sci 61(6), 2881-2888 (2014).

[25]H. Gao, D. Ahsanullah, R. Baumann, and B. Gnade, *Radiation Effects Data Workshop* (2022), 1-6.

[26]S. Stoffels, M. Mélotte, M. Haussy, R. Venegas, D. Marcon, M. V. Hove, and S. Decoutere, IEEE Trans. Nucl. Sci 60(4), 2712-2719 (2013).

[27]S. Bazzoli, S. Girard, F. Cavrois, J. Baggio, P. Paillet, and O. Duhamel, *in Proc. 9th Eur. Conf. Radiat. Effects Compon. Syst* (2007), 565-569.

[28]P. Kupsc, A. Javanainen, V. F. Cavrois, M. Muschitiello, A. Barnes, A. Zadeh, J. Calcutt, C. Poivey, H. Stieglauer, and K. O. Voss, IEEE Trans. Nucl. Sci 65(2), 732-738 (2018).

[29]Q. K. Yu, Y. Sun, Z. Wang, B. Mei, X. L. Li, H. Lv, P. Li, L. Luo, M. Tang, and P. Wen, *in Proc. Int. Conf. Radiat. Effects Electron. Devices* (2018), 1-3.

[30]A. Javanainen, V. F. Cavrois, A. Bosser, J. Jaatinen, H. Kettunen, M. Muschitiello, F. Pintacuda, M. Rossi, J. R. Schwank, M. R. Shaneyfelt, and A. Virtanen, IEEE Trans. Nucl. Sci 61(4), 1902-1908 (2014).